D2.5 - REPORT ON SPECIFICATIONS FOR EXPERIMENTAL (AAWT/UOB) AND NUMERICAL STUDIES ON POROUS SLAT NOISE IN WP4

Document authors	
Hasan Kamliya Jawahar	UoB
Mahdi Azarpeyvand	UoB
Document contributors	
Christophe Schram	VKI
Daniele Ragni	TUD
Alejandro Rubio Carpio	TUD
Gareth Bennett	TCD
Michael Pott-Pollenske	DLR
Matthias Meinke	RWTH
Marc Terracol	ONERA
Vincent Fleury	DAV

Abstract

In this report the specifications for the preliminary experimental and numerical studies of slat noise reduction using porous materials, which will be carried out in a later stage (T4.1) of the INVENTOR project are described. Specifications on the following subjects are given:

- the characterisation of the porous materials by TUD
- the outline of the preliminary experiments by VKI
- the manufacturing of the porous materials by TCD
- the outline of the experimental test in the aeroacoustic wind tunnel (AAWT) at UoB
- the setups for the numerical tests for the VKI experiments by RWTH

Keywords : Slat noise reduction, porous materials.

1 Information Table

Project information	
PROJECT ID	860538
PROJECT FULL TITLE	INnoVative dEsign of iNstalled airframe componenTs for aircraft nOise Reduction
PROJECT ACRONYM	INVENTOR
FUNDING SCHEME	RIA – Research and Innovation Action
START DATE OF THE PROJECT	1st May 2020
DURATION	48 months
CALL IDENTIFIER	H2020-MG-2018-2019-2020

Deliverable information	
DELIVERABLE No AND TITLE	D2.5 - Report on specifications for experimental (AAWT/UoB) and numerical studies on porous slat noise in WP4
TYPE OF DELIVERABLE[1]	Report
DISSEMINATION LEVEL[2]	Public
BENEFICIARY NUMBER AND NAME	14 TUD, 12 VKI, 1 ONERA, 10 RWTH, 13 UoB, 8 TCD, 5 DLR, 3 DAV
AUTHORS	Hasan Kamliya Jawahar, Mahdi Azarpeyvand
CONTRIBUTORS	Christophe Schram, Matthias Meinke, Daniele Ragni, Alejandro Rubio Carpio, Gareth Bennett, Michael Pott-Pollenske, Marc Terracol, Vincent Fleury
WORK PACKAGE No	2
WORK PACKAGE LEADER **WP LEADER VALIDATION DATE**	Vincent Fleury, DAV, 07/06/2021
COORDINATOR VALIDATION DATE	Eric Manoha, ONERA, 08/07/2021
Coordinator signature	

1 Use one of the following codes: R=Document, report (excluding the periodic and final reports)
DEM=Demonstrator, pilot, prototype, plan designs
DEC=Websites, patents filing,press & media actions, videos, etc.
OTHER=Software, technical diagram, etc.

2 Use one of the following codes: PU=Public, fully open, e.g. web
CO=Confidential, restricted under conditions set out in Model Grant Agreement
CI=Classified, information as referred to in Commission Decision 2001/844/EC.

2 Table of Contents

1 Information Table 2

2 Table of Contents 3

3 Introduction 4

4 Porous material selection 5

4.1 Diamond-lattice design by TUD 5

4.2 Poly-urethane foam inserts by DLR 6

5 Characterization and modelling of porous materials 7

5.1 Global strategy 7

5.2 WAABLIEF test set-up 7

5.3 Numerical activities by RWTH 9

5.4 Numerical activities by VKI 10

6 Specifications of the F16 model for the AAWT tests 10

6.1 New wing trailing edge 10

6.2 Porous slat inserts on the F16 model 11

7 Specifications of AAWT wind tunnel test 14

7.1 Test facility 14

7.2 Measurement techniques 15

7.2.1 Beamforming measurements 15

7.2.2 Directivity measurements 16

7.2.3 Surface pressure measurements 16

7.3 Test parameters 16

7.4 Time Schedule and Action list 16

8 References 17

3 Introduction

The objective of INVENTOR is to reduce airframe noise, namely landing gear noise and high-lift device noise. Acoustic objectives were derived from targeted aircraft noise reduction level at approach in certification (-1 EPNdB) down to individual airframe systems, see Deliverable D2.1 [2]. As explained in this document (D2.1), to reach 1 EPNdB gain at aircraft level, noise reduction is required on every systems (slat, flap, landing gears and ideally on engines too). For slats in particular the objectives are recalled in Table 1. Two test cases are considered, either state-of-the-art engines, or engines with 0.5 dB noise reduction. The targeted frequency ranges correspond to full-scale and approach conditions. Transposition to reduced scale and other flow velocities follows a conventional Strouhal number law with reference features recalled in Table 2. The high-lift device configuration along with the angle of attack at approach are also provided.

A/C platform	**Frequencies of prime interest (1/3rd octave freq.)**	**Emission angles of prime interest**	**Targeted slat noise reduction level**	
			State-of-the-art engine	**0.5 dB engine noise reduction**
Generic SMR A/C	< 800Hz	20°-160°	1 EPNdB(*)	1 EPNdB(*)
Generic business jet	[63Hz – 800Hz]	20°-160°	3 dB(**)	2 dB(**)

Table 1. Targeted slat noise reduction levels.
(*) Same reduction expected in the dB metrics for all frequencies and emission angles.
(**) The same level of noise reduction is assumed on all other airframe noise sources (installed LG and Flaps).

	Commercial Short-Medium Range aircraft	**Generic Business Jet**
Reference length (slat chord)	0.45 m	0.36 m
Reference velocity (approach speed)	72 m/s	75 m/s
HLD configuration	Slat: 30° / Flap: 40°	Slat: 27° / Flap: 40°
A/C angle of attack	5°	5°

Table 2. Reference features for the slat of the generic business jet and commercial SMR aircraft.

The present report, Deliverable D2.5, describes the progress and planning for the application of porous materials for slat noise reduction. Various porous samples will be manufactured using additive manufacturing technology and their acoustical characteristics will be measured in a small-scale test bench (WAABLIEF) to contribute to the development of numerical models in CFD solvers. Then, a range of surface inserts based on these materials will be manufactured and adapted to the hybrid F16 model of DLR, which represents a wing with slat, but no flap, nor sweep (2D model) in the present case. This small-scale model will be tested with and without such treatments in the UoB aeroacoustic facility AAWT in order to check the actual capability of the considered treatments.

4 Porous material selection

4.1 Diamond-lattice design by TUD

Porous slat inserts will be 3D printed based on a diamond-lattice design of TUD, however, additional designs of TCD and one set of foam inserts from DLR will also be tested. The proposed open-cell porous materials of TUD are all based on the three-dimensional repetition of diamond-lattice unit cells (Figure 1). This cell typology has been previously employed in aeroacoustic research for low trailing-edge noise applications [2, 3]. Three different materials are proposed to study the effect of locally changing properties such as permeability on the flow field at the slat cove region. The porous materials are created by scaling the cell size d_c to 3.5, 4.5 and 6.4 mm, as shown in Figure 1. The minimum cell size is given by manufacturing constraints, i.e. it guarantees a satisfactory outcome of the additive manufacturing process and a manageable CAD file. The maximum cell size allows allocating approximately one full cell at the slat porous insert leading-edge. The employment of porous inserts with different properties is aimed at modifying the flow field in the slat cove region, thus decreasing noise generation. The porosity of all three micro-structures is of 62%. The higher bound for the permeability of the samples is 10^{-8} m^2. For comparison, a sketch including squared samples, created by periodically repeating unit cells with the above defined cell diameters, is shown in Figure 2. Porous materials based on a similar diamond-lattice cell have also been proposed in the framework of WP3 for low-noise landing gear applications. In such context, porous fairings with cell diameters ranging between 2.5 and 6.4 mm are proposed; these solutions impose different pressure drops across the fairing, allowing to effectively control the flow field within the landing–gear axle region.

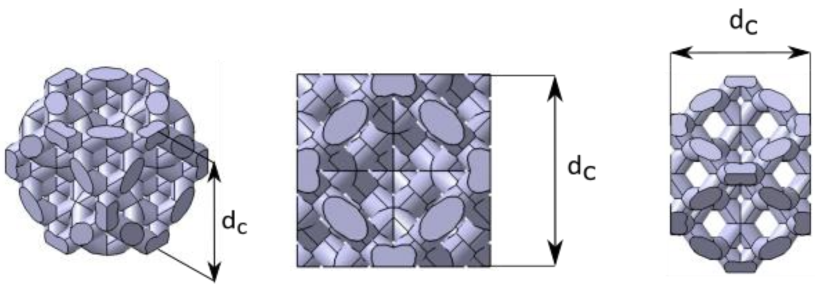

Figure 1: Sketch of the diamond-lattice unit cell. Isometric view (left). Front/side/top view (middle). View from a plane slanted 45 degrees (right).

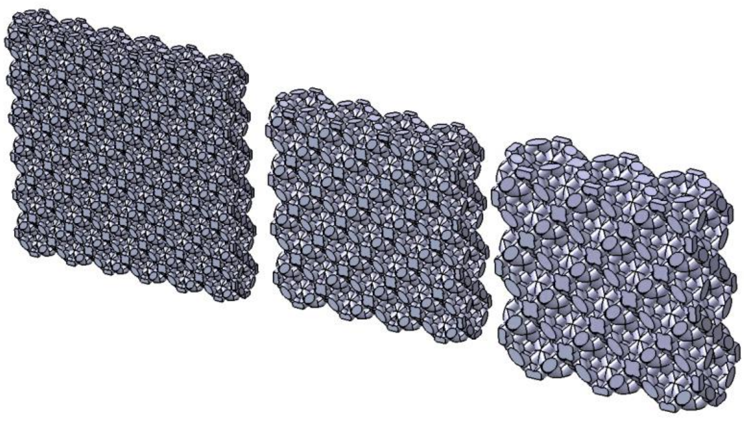

Figure 2: Isometric view of squared samples created with the proposed unit cells. 21x21x3.5mm^3 sample with cell size of 3.5 mm (left). 18x18x4.5mm^3 sample with cell size of 4.5 mm (middle). 19x19x6.4mm^3 sample with cell size of 6.4 mm (right).

4.2 Poly-urethane foam inserts by DLR

DLR will provide a set of open cell poly-urethane foam inserts. In terms of shape and size, the DLR inserts are similar to those fabricated by TCD. The only difference is insert's length, which is 300 mm and thus fits to the length or span of one cavity.

The design is based on an outer shell bended from metal. This shell fits to the cavity's shape. The inner volume of the shell is filled with open cell foam. This foam layer is meant to attenuate unsteady pressures. A thin wire mesh facing sheet closes the liner towards the slat cove flow. The assembly is depicted in Figure .

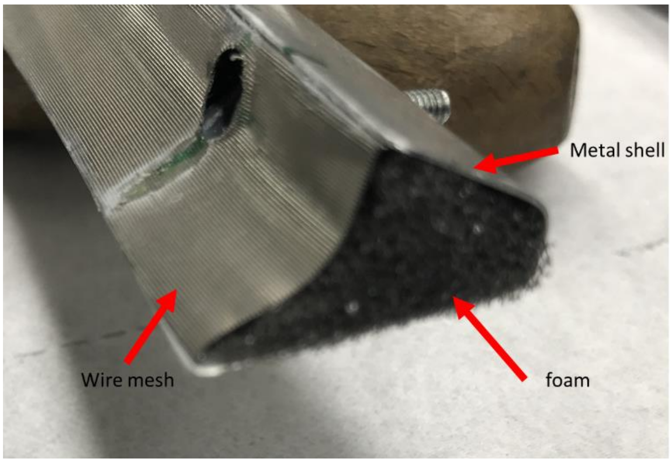

Figure 2.1: Assembly of porous insert

The acoustic attenuation characteristic of the foam is provided by the manufacturer in term of the attenuation as measured in an impedance tube according to ISO 10534-2 (Figure 2). The attenuation provided by the thin insert can be best compared to the data represented by the black curve in the diagram in Figure 2.2.

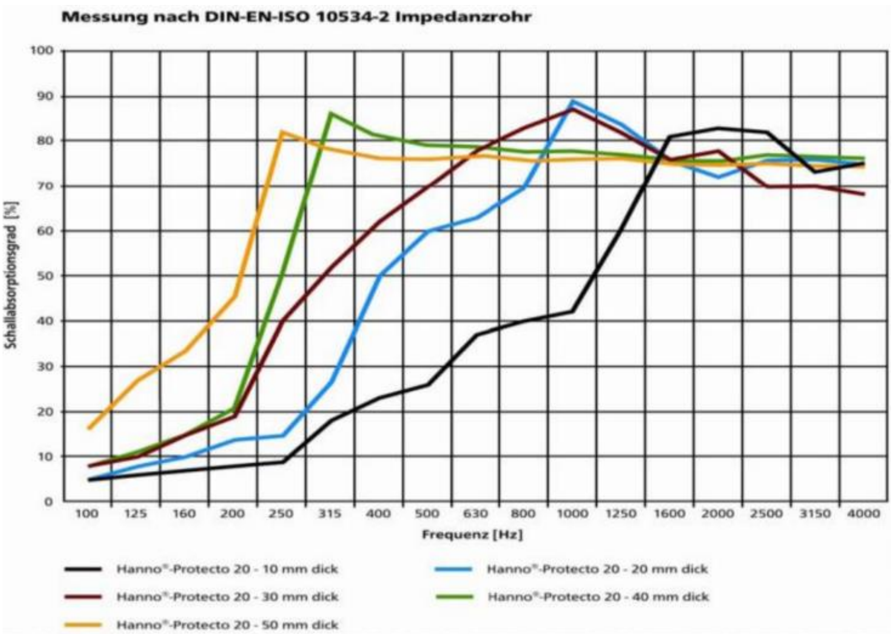

Figure 2.2: Sound attenuation of HANNO Protecto20 foam, courtesy of HANNO® Werk GmbH&Co

The wire mesh, covering the poly-urethane foam, consists of woven stainless steel and is the same as provided for the characterizations in B2A and WAABLIEF, see Section 5. The porosity is about 40% (open area). Further specifications are given in Deliverable 2.2.

5 Characterization and modelling of porous materials

5.1 Global strategy

In Task 4.1, RWTH will carry out scale-resolved numerical simulations of the flow and acoustic field of the DLR's unswept F16 model slat-wing mockup without and with porous treatment. Such simulations require calibrating a numerical model of the porous treatment in the CFD solver, which requires the *a priori* determination of the following characteristics of the porous materials:

1. Mean-velocity profiles, Reynolds stresses, streamwise integral length scale evaluated at about $10\delta_{BL}$ upstream of the porous insert.
2. Mean-velocity profiles, Reynolds stresses, streamwise integral length scales along the porous insert.
3. Surface pressure spectra on the porous insert and at the bottom of the cavity where the insert is placed.

These characteristics will be first measured on planar samples with grazing flow at VKI in the WAABLIEF facility (see Section 5.2), and this configuration will be used by RWTH for validation computations.

In the same Task 4.1, VKI will use a FEM solver (Simcenter 3D) to compare the acoustic response of the UBRI wing-slat mock-up without/with an equivalent acoustic impedance boundary condition on the surface of the porous patch for a generic source (to be defined). In order to determine the required acoustic normal impedance boundary condition, a Kundt-tube experimental mock-up at VKI or UBRI will be used by inserting the same porous materials that will be fitted in the UBRI mock-up. Then, the grazing flow characterization will be "in-situ" measured at WAABLIEF with the planar samples inserted in the lower wall of the facility. The characterization will be performed by measuring the local velocity fluctuations near the surface of the liner with hot-wire anemometry (HWA) or particle image velocimetry (PIV), while the pressure fluctuations will be measured with a remote microphone probe. Subsequently, these quantities will be used to make an attempt to model the acoustic grazing impedance in Simcenter 3D. Afterward, the measurements will be compared with Simcenter 3D acoustic simulations.

5.2 WAABLIEF test set-up

This WAABLIEF test rig is an open-circuit, suction type, low-speed wind tunnel with a transparent square test section having a dimension of 0.25 x 0.25 m2 that is dedicated to the characterization of porous materials with grazing flows. Three porous test samples designed by TUD with two different cell sizes (namely 3.5, and 4.5, mm) will be investigated in a liner configuration, as shown in Figures 3 and 4. The dimensions of the sample are reported in Figure 3. The width (along the y-axis with reference to the coordinate system in the figure) of the insert has been designed in order to be larger than $3\delta_{BL}$, δ_{BL} being the expected boundary layer thickness. This extension allows considering the flow field over the material at $y = 0$ as statistically two-dimensional. The length (along x) and the thickness (along z) have been designed in order to fit an existing allocation placed at the bottom side of the test section.

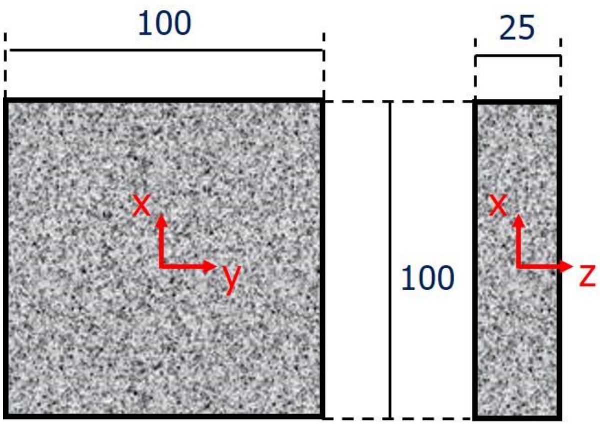

Figure 3: Dimensions of the porous test sample. The flow is directed along x. The dimensions are expressed in mm.

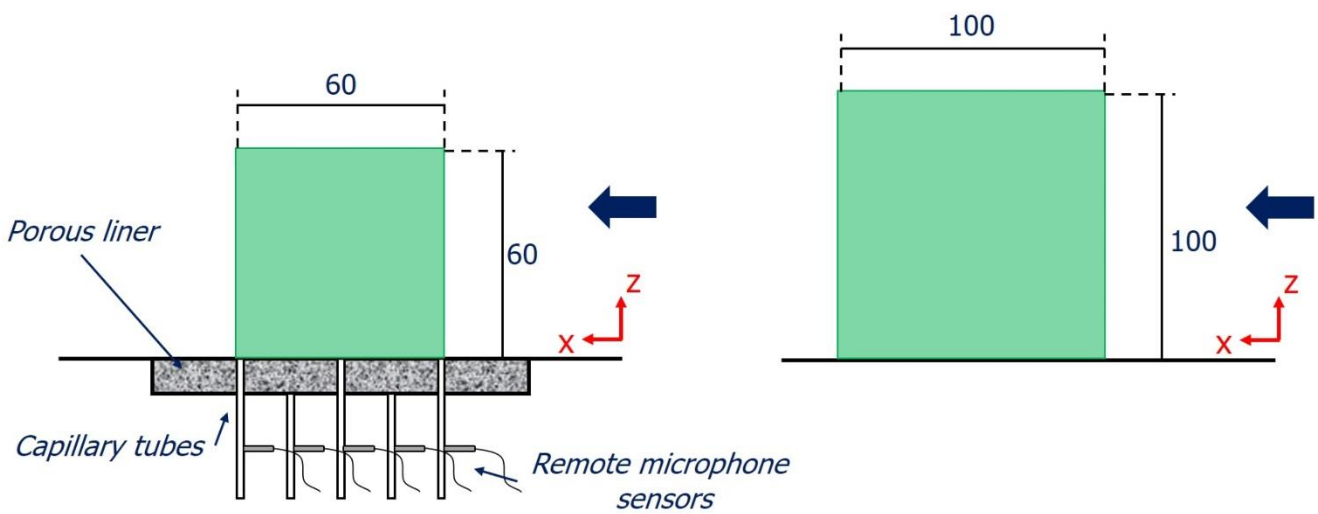

Figure 4: Measurements planes for the 2D-3C PIV. The dimensions are expressed in mm.

Three flow velocities at the test-section inlet will be considered, namely 15, 25, and 30 m/s. 2D-3C PIV measurements on two different x-z cross-sections (see Figure 4) will be performed in order to provide the quantities described in points 1 and 2 above. Preliminary tests have been performed in order to assess the uniformity of the seeding particles. The surface of the porous insert will be designed in order to minimize the reflections due to the laser. Moreover, the sample and the cavity where this is placed will be equipped with 5 capillary tubes connected to remote microphone sensors uniformly distributed along the streamwise direction in order to measure the quantities described in point 3. The locations of the remote microphone sensors at the liner surface and at the bottom of the cavity are shown in Figure 4.

5.3 Numerical activities by RWTH

RWTH will perform numerical simulations to complement the experiments conducted by VKI of a grazing flow over a porous liner. The objective is twofold, first to calibrate the porous flow model for later use in WP4, and to shed light on the near wall turbulence alteration caused by a permeable surface.

The experimental setup will be simulated as a spatially evolving turbulent boundary layer over a flat plate, as sketched in Figure 5, by solving the volume averaged Navier-Stokes equations for the flow field using a finite-volume method based on an advective upstream splitting method (AUSM) in conjunction with the monotone upstream centred scheme for conservation laws (MUSCL) for the inviscid fluxes and a cantered discretization for the viscous fluxes. Both spatial formulations are second-order accurate. The LES is based on the monotone integrated LES (MILES) ansatz, in which the low dissipation of the numerical methods replaces an explicit subgrid scale model. A low-storage explicit 5-stage Runge-Kutta method for the time integration also of second-order accuracy is used for the time integration.

Among others the porous model includes a momentum transfer condition formulated as jump conditions across the fluid-porous interface. The tangential component of the jump for the stress, which acts as a singular force, depends on an undetermined parameter. This changes the velocity gradient and thus the turbulent production as well as the boundary profiles. By fitting the turbulent statistics to those of the measurements the empirical parameter will be determined. In cooperation with VKI the spanwise extension of the porous insert was chosen to be roughly three times the expected boundary layer thickness to minimize side effects in the mid-plane. This allows the use of of periodic boundary conditions in the spanwise direction in the simulations. To ensure comparability with the measurements it is important to prescribe inflow conditions in the numerical simulation, which match the characteristics of the boundary layer upstream of the porous insert in the WAABLIEF facility. This is accomplished by the turbulent inflow generation technique by Lund et al. [4], where the turbulent boundary layer profile at a downstream plane is rescaled to the target boundary layer momentum thickness and friction Reynolds number measured in the experiment and introduced at the inlet. The flow conditions at station 1 and 2, see Fig. 5, are summarized in table 1, which are also documented in [5].

The freestream flow velocities of 15 m/s and 25 m/s lead to the momentum thickness Reynolds numbers of $Re_\Theta = 3219$ and $Re_\Theta = 5125$ at the test station. A wall spacing of the structured mesh with $\Delta y(y^+\approx1)=2.4e\text{-}5$ m and $\Delta y(y^+\approx1)=1.5e\text{-}5$ m will be used. The post-processing of the data will include one-point, second-order statistics (i.e. Reynolds stress tensor), two-point correlations and the pressure signals at the locations of the microphones.

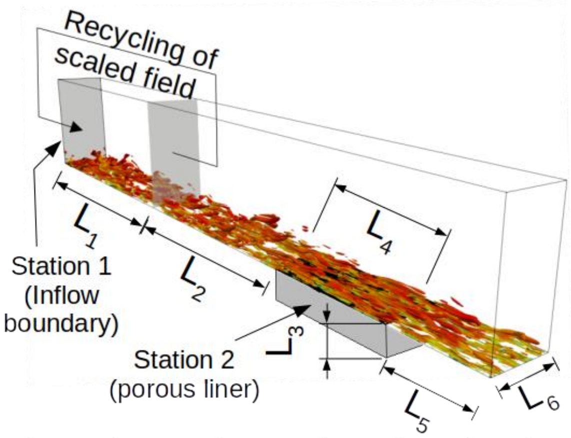

L_1	L_2	L_3	L_4	L_5	L_6
$12\delta_{99}$	0,45m-L_1	0,025m	0,1m	$3\delta_{99}$	$3\delta_{99}$

Figure 5: Sketch of the grazing flow setup with the porous insert and turbulent flow structures. Station 1 corresponds to the inflow plane, station 2 to the center of the porous insert.

		Station 1		Station 2	
U_e	[m/s]	14.95	25.94	15.43	26.28
δ_{99}	[m]	19.0×10^{-3}	20.0×10^{-3}	30.0×10^{-3}	31.7×10^{-3}
θ	[m]	2.23×10^{-3}	2.18×10^{-3}	3.13×10^{-3}	2.92×10^{-3}
Re_θ	[-]	2218.4	3778.9	3219.3	5125.8

Table 1: Boundary layer characteristics of WAABLIEF facility for two inlet velocities [5].

5.4 Numerical activities by VKI

In a first step, the acoustic grazing impedance measurements with Kundt-tube will be compared with Simcenter 3D acoustic simulations. After determining the impedance boundary conditions for different porous materials, the simulation of the UBRI mock-up will be performed with Simcenter 3D to investigate the dependence of acoustic attenuation due to porosity on the impedance.

The noise regeneration due to the added roughness will be investigated using Amiet’s model. The required input for the model is the turbulent boundary layer at the level of the slat TE of the UBRI mock-up after the porous patch, which will be obtained either through measurements by UBRI or numerical simulations by RWTH. The output of the model will be to assess how the slat TE noise would be affected by the porous liner.

6 Specifications of the F16 model for the AAWT tests

6.1 New wing trailing edge

As part of subtask 4.1.4 it has been decided to modify the existing DLR's unswept F16 model to have the trailing edge replaced with a “Valiant like” trailing edge for tests at UoB (porous slats) and NLR (low noise slat tracks). The details of the wing model with the modification have been detailed in report D2.3 [6] by NLR. The modifications to the DLR F16 model are shown in Fig. 6. Although the model uses several tracks to position the main element and slat, only the two slat tracks that falls outside the test section of 530 mm will be used to eliminate slat track noise and in order to capture the possible noise reduction capability of the porous slat inserts. Previous studies at UoB have followed similar strategy and there has not been any issues with structural deformation for velocities up to 40 m/s as the test section is fairly small. Moreover, the side plates also act as placeholders for the slat and maintain the position of the slat.

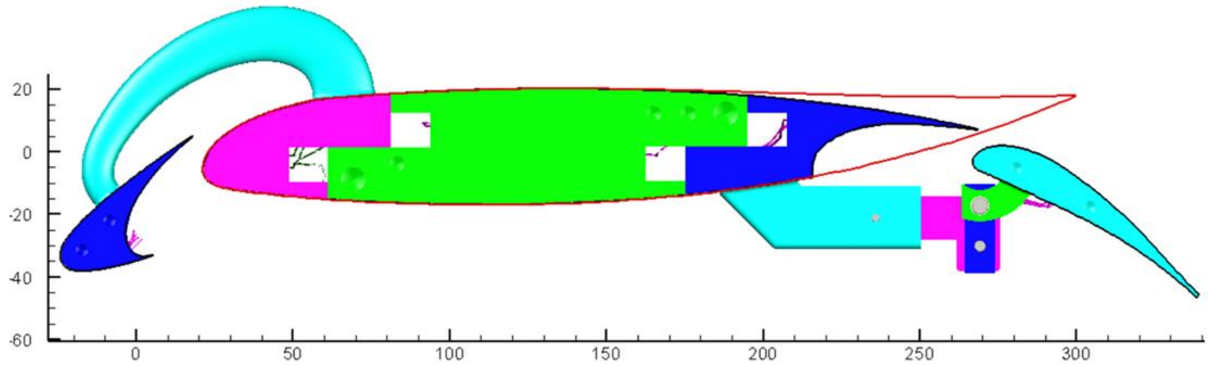

Figure 6: Cross section of original F16 model and modification of the main element TE shown in red.

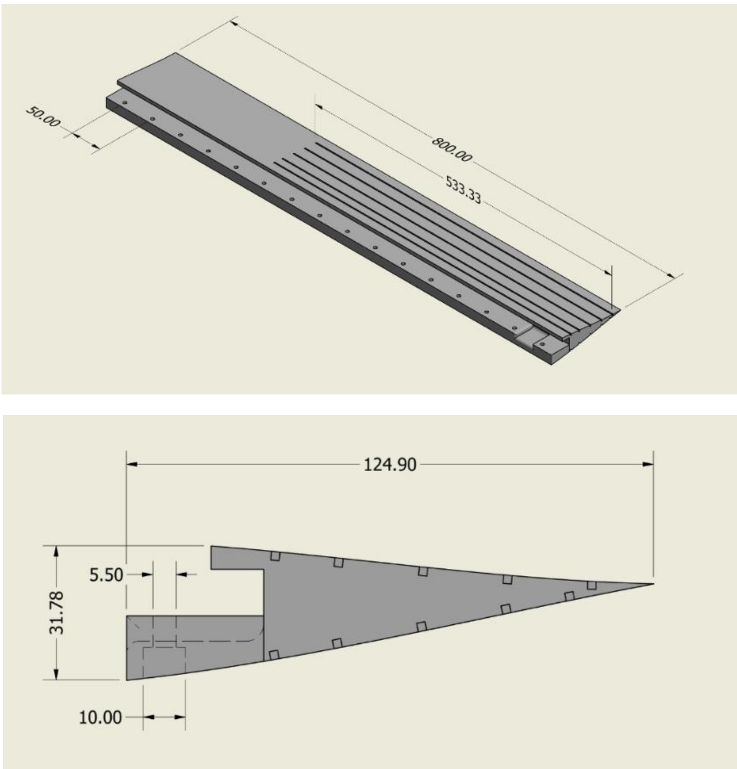

Figure 7: Trailing edge design manufactured at UoB.

The "Valiant like" trailing edge for tests at UoB and NLR designed by ONERA through detailed numerical simulations reported in D2.3 has been manufactured by UoB using aluminum and EDM machining. The trailing edge of length 800 mm was made using 4 pieces of length 200 mm stacked together. A schematic of the preliminary design for the trailing edge is shown in Fig. 7. The final model has pins between the 4 pieces to align them accurately. Brass tubes were used for pressure taps and were glued to the surface using epoxy and sanded later for smooth surface finish. The trailing edge model has 10 slots for the brass tubes bent inward so that they will not interfere with the attachments that will be used by NLR to further extend the model span length. The trailing edge has been successfully integrated in to the F16 high lift system.

6.2 Porous slat inserts on the F16 model

The optimal porous materials suggested by TUD will be printed by TCD for experimentation at UoB and later at F2. The placement of the porous insert, as suggested by DLR, is shown in Fig. 8. In Fig.

8 (a) the original slat insert proposal is shown. There were some difficulties in printing the very thin section of the porous insert, which is only 0.5 mm thin and it was agreed that would have negligible acoustic benefit. Figure 8 (b) shows a revised proposal (in blue) where the thin section is removed, and instead greater volume is dedicated at the stagnation point. Figure 9 shows the solid model of insert iteration 2 using the 6.4mm Diamond-lattice cell. The model was designed to ensure maximum material at the thin edge to ensure strength and continuity and sleeves were incorporated into the design around the fixture holes to ensure strength. 3D printed parts of this design using an MSLA method are shown in Fig. 10. The porous inserts are 150 mm long and four inserts would be required for the slat as shown in Fig. 11. It was realized that the carrier plate design which would need to be glued to the insert would not work as the glue would be absorbed by the insert, rendering it inefficient. Instead, it was decided to remove the carrier plate from the design, which has the added benefit of allowing the porous insert to be deeper which should improve the acoustic potential. A solid model of insert iteration 3 is shown in Fig. 12. Also shown is a 3D printed box which will be 3D printed in order to protect the inserts while being shipped to UoB. The inserts will be screwed into the box using M3 screws as per the slat.

The 6.4 mm diamond-cell lattice has been used to allow the design to be finalized due to the ease of 3D printing but it is understood that a smaller lattice of sizes 3.5, and 4.5 mm will be required in the INVENTOR, which will be used for the tests at VKI and for numerical simulation at RWTH. An attempt to create a porous slat cove filler with cell diameter of 2.5 mm was not successful due to software/hardware limitations, i.e., the corresponding CAD file was too heavy to be handled by traditional CAD software such as Solidworks/CATIA. Figure 13 shows some finer lattice structures printed by TCD in the AERIELIST project : lattice structures of these types will be provided by TCD if time allows.

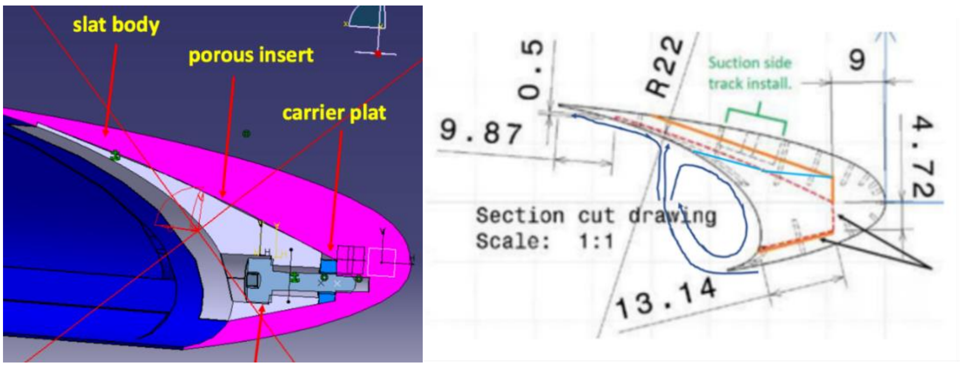

(a) Insert iteration 1 **(b) Insert iteration 2**

Figure 8: Cross section of slat showing insert proposals.

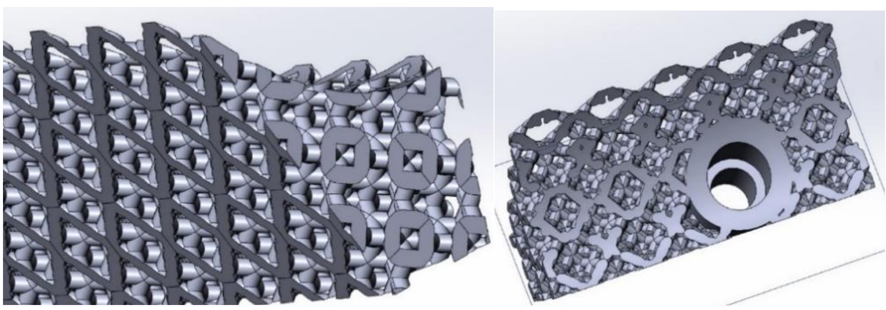

Figure 9: Short section of Insert iteration 2 with 6.4 mm diamond-lattice. Location of cell is optimized to provide most material at thin edge.

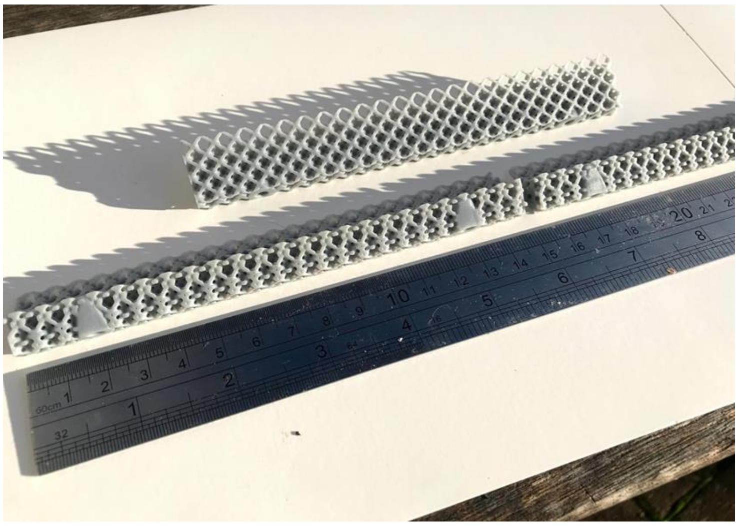

Figure 10: Preliminary test 3D prints from TCD: 6.4 mm diamond-lattice, Insert iteration 2.

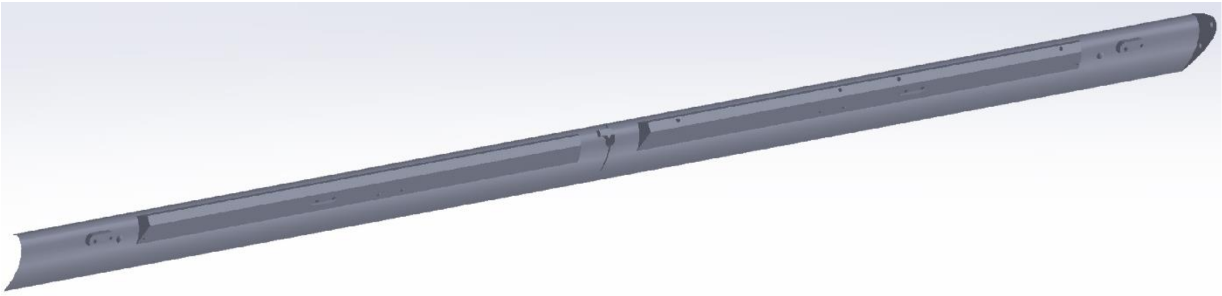

Figure 11: Slat without inserts. Insert iteration 3. No carrier plate to allow for a deeper insert.

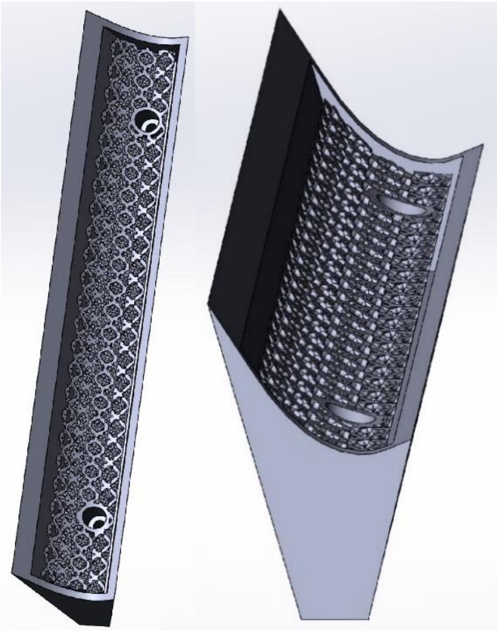

Figure 12: Insert iteration 3. 150 mm long using 6.4 mm diamond-cell lattice. The insert is shown located in a container which will be 3D printed in order to house the insert so that it will not be damaged in shipping.

Figure 13: Samples of lattice structures printed by TCD in the AERIELIST project.

7 Specifications of AAWT wind tunnel test

7.1 Test facility

The F16 high-lift model with the modified wing trailing edge will be tested using the Kevlar test section at the University of Bristol to minimize the effect of open jet on the aerodynamic and acoustic characteristics of the high-lift airfoil. The aeroacoustic wind tunnel in which the Kevlar-walled test section is installed has a 3.2 m gap between the nozzle outlet and the collector inlet. The Kevlar-walled test section, as seen in Fig. 14, has a total length of 1500 mm leaving a distance of approximately 1700 mm to the inlet plane of the collector. The length of the tensioned Kevlar cloth is long enough such that all noise from the aerofoil passes through the Kevlar and not any wind tunnel free shear layer until the noise reaches the far field directional microphone array. Moreover, considering the length of the Kevlar section in the UoB facility, the effect of boundary layer will be minimal, and efforts will be made to correct the far field noise data for sound absorption caused by the Kevlar. Acoustic tests for the sound absorption effects of Kevlar wall has already been carried out and the relevant corrections can be applied. The distance from the end of the test section to the collector allows the jet to sufficiently expand before it is channelled into the first silencer after the collector and hence ensures the regenerative noise of the silencer does not exceed the present background noise. The test section shares its internal dimensions of 775 mm height and 500 mm width with the exit dimensions of the nozzle of the aeroacoustic facility. The structure of the section is made from Bosch Rexroth struts and connectors, and the flow wetted surface area of any strut is smooth and without any mounting slots to avoid any erroneous noise sources. Three windows made from Perspex and Sapele wood are located on each side and the Perspex of the first window has a circular cut-out with a diameter of 500 mm to mount the test object via a side plate. Additionally, the inside of the circular cut-out is lined with 0.1 mm thick PTFE Teflon tape by 3M, to reduce the friction between the side plate and the window. The 300 mm long second and third windows allow the insertion of intrusive measurement techniques, such as hot-wire anemometry. All windows are sealed on all four sides by means of polychloroprene rubber (Neoprene) strips, which are compressed when installing each window, and hence no air leakages can occur. Furthermore, all internal gaps as well as the connection to the wind tunnel nozzle have been covered with insulation tape to ensure no spurious noise from any steps or gaps is created. The aerodynamic and aeroacoustic tests will be carried out for free-stream velocities ranging from 20 to 40m/s.

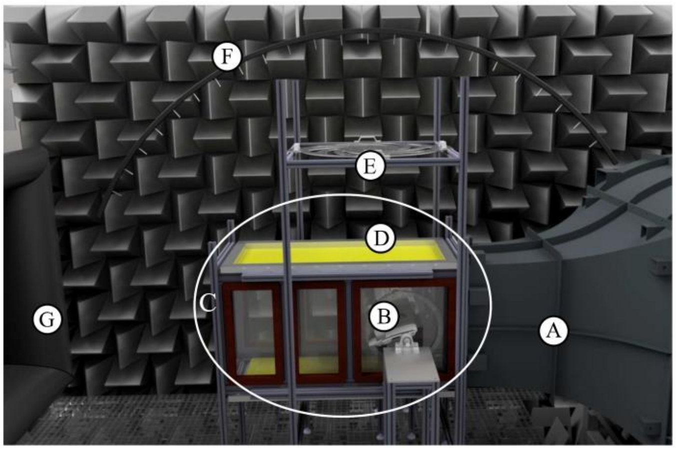

Figure 14: Overview of the Kevlar-wall test section with mounted high-lift device inside the anechoic chamber; (A) contraction nozzle, (B) Modified F16 high-lift device, (C) test section, (D) Kevlar tensioning frame, (E) beamforming array, (F) far-field microphone arc, (G) collector.

7.2 Measurement techniques

7.2.1 Beamforming measurements

In order to locate the noise sources from the high-lift model, the UoB beamforming array will be used. The beamforming array is made from 83 microphones (Panasonic WM-61A) distributed along 9 arms with 9 microphones each, and additional microphones in the center of the array, as illustrated in Fig. 15. For the present study, the center of the beamforming array will be aligned with the slat cusp and positioned at a distance of 1 m above the test section. For maximum transparency the microphone supports were manufactured using wire mesh as shown in Fig. 15.

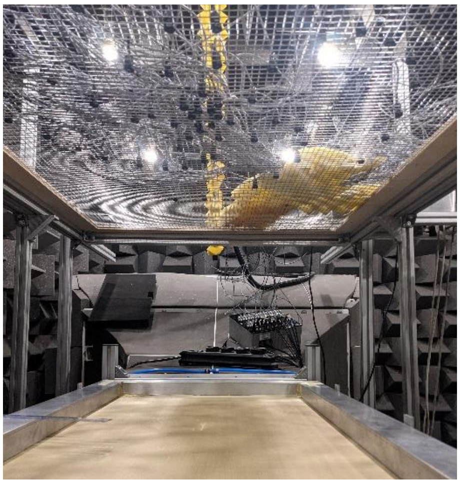

Figure 15: Beamforming array mounted above the Kevlar-walled test section.

7.2.2 Directivity measurements

In order to measure the directivity of the slat noise sources from the high-lift model a microphone arc with 23 G.R.A.S. 40PL microphones (see Fig. 14), located at a distance of $r = 1.75$ m, spanning from polar angle of $\theta = 30°$ to $\theta = 140°$, spaced at a regular interval of $\theta = 5°$. A polar angle of $\theta = 0°$ denotes a microphone aligned in parallel with the free stream flow vector, but pointing upstream. The G.R.A.S. 40PL microphones have a built-in amplifier and are operated via IEPE from the National Instruments data acquisition system. The microphones have been calibrated prior to commencing the measurements using a G.R.A.S. 42AA pistonphone calibrator.

The microphone arc allows direct measurements of the far-field noise levels as well as the noise directivity, for frequencies in excess of $f = 160$ Hz, corresponding to the cut-off frequency of the anechoic chamber. In order to avoid reflections from the arc itself and noise contamination at mid to high-frequencies, the arc is covered in acoustic foam.

It is important to note that directivity and beamforming measurements will be carried out separately.

7.2.3 Surface pressure measurements

Both steady and unsteady surface pressure over the modified F16 airfoil will be acquired as part of the experimental campaign at UoB. The static surface pressure measurements will be carried out using the pressure ports in the high-lift airfoil that are detailed in report D2.3 [6]. The new trailing-edge part will also be instrumented at UoB to enable adequate pressure measurement over the full chord of the main component. The unsteady surface pressure measurements in the slat cove region will be carried out using the Kulites, which are pre-installed in the F16 airfoil by DLR (12 Kulites, 4 in spanwise orientation, 8 in one chordwise cross-section). Both the far-field measurements and the near-field surface pressure measurements will be carried out simultaneously.

7.3 Test parameters

The tests will be carried out for 2 different angles of attack at three freestream velocities of 20, 30 and 40 m/s. The two angles of attack will be determined after thoroughly characterizing the F16 HLS in the Kevlar wind tunnel at UoB. Three porous slat inserts along with the baseline configuration designed by TUD will be tested at UoB fitted on the modified F16 HLS. The noise measurements will be acquired using National instruments system fixed with several PXIe 4499 sound and vibration cards. The acoustic measurements will be carried out at a sampling frequency of 102.4 kHz with a sampling duration of 30 s.

7.4 Time Schedule and Action list

- The 3D prints were prepared by TCD and they are ready to be tested at UoB.
- The high-lift airfoil fully fitted with Kulites has to be sent to UoB with the necessary amplifiers before the tests could begin by October first week.
- UoB has reserved approximately 2-3 weeks for the porous slat inserts tests in INVENTOR. The initial planning assumed tests between July and August 2021. However, due to planning constraints linked to sharing the model with other tests in INVENTOR (at NLR in T4.2 for slat tracks for 2 weeks in mid-July) and outside INVENTOR (at DLR/NWB for a DLR-ONERA cooperation, for 2 weeks in mid-September) the UoB tests are now more likely to be achieved

in October 2021. Note that this planning shift should not dramatically affect the specifications of the future INVENTOR tests of porous slats and low noise slat tracks in ONERA/F2 (T4.3), to be achieved in April-May 2022.

8 References

[1] Aline Scotto, Vincent Fleury, *Report On Specification On Acoustic Reduction*, INVENTOR D2.1.

[2] C. Teruna, F. Avallone, D. Casalino, D. Ragni, A. Rubio Carpio, F. Manegar, T. Carolus. *Trailing Edge Noise Reduction with Permeable Materials: Description of Noise Scattering Mechanism*. September 2019, 23rd Workshop of the Aeroacoustics Specialists Committee of the CEAS at Roma Tre University, Rome, Italy.

[3] A. Rubio Carpio, S. Luesutthiviboon, R. Hedayati, F. Avallone, D. Ragni, M. Snellen, S. van der Zwaag. *3D-printed Permeable Trailing Edges for Broadband Noise Abatement*, September 2019, 23rd Workshop of the Aeroacoustics Specialists Committee of the CEAS at Roma Tre University, Rome, Italy.

[4] T. S. Lund, X. Wu, K. D. Squires. *Generation of turbulent inflow data for spatially-developing boundary layer simulations.* Journal of computational physics, 140(2), 233-258, 1998.

[5] N. Van de Wyer, A. Zapata, D. Nogueira, C. F. Schram. *Development of a test rig for the measurement of turbulent boundary layer wall pressure statistics*. In 2018 AIAA/CEAS Aeroacoustics Conference (p. 3122).

[6] Evelien van Bokhorst, *Report On Specifications For Preliminary Experimental (AWT/NLR) and Numerical Studies on Slat Track Noise in WP4,* INVENTOR D2.3.